

Oscillations in the Habitable Zone around α Centauri B

Duncan Forgan ^{1*}

¹*Scottish Universities Physics Alliance (SUPA), Institute for Astronomy, University of Edinburgh, Blackford Hill, Edinburgh, EH9 3HJ, Scotland, UK*

Accepted

ABSTRACT

The α Cen AB system is an attractive one for radial velocity observations to detect potential exoplanets. The high metallicity of both α Cen A and B suggest that they could have possessed circumstellar discs capable of forming planets. As the closest star system to the Sun, with well over a century of accurate astrometric measurements (and α Cen B exhibiting low chromospheric activity) high precision surveys of α Cen B’s potential exoplanetary system are possible with relatively cheap instrumentation. Authors studying habitability in this system typically adopt habitable zones (HZs) based on global radiative balance models that neglect the radiative perturbations of α Cen A.

We investigate the habitability of planets around α Cen B using 1D latitudinal energy balance models (LEBMs), which fully incorporate the presence of α Cen A as a means of astronomically forcing terrestrial planet climates. We find that the extent of the HZ is relatively unchanged by the presence of α Cen A, but there are variations in fractional habitability for planets orbiting at the boundaries of the zone due to α Cen A, even in the case of zero eccentricity. Temperature oscillations of a few K can be observed at all planetary orbits, the strength of which varies with the planet’s ocean fraction and obliquity.

Key words:

astrobiology, planets and satellites: general, radiative transfer

1 INTRODUCTION

There are currently 755 known extrasolar planets, spanning a large parameter space in orbital elements and in planetary properties¹. The question of planet formation in binary systems is an important one, as a large fraction of solar type stars are born in binary or multiple star systems (Duquennoy & Mayor 1991). The majority of these systems are wide S-type binaries, where the secondary orbits at distances of over 100 au from the planetary system. At the time of writing, around 15% of planets have been detected in binary star systems Desidera & Barbieri (2007). In S-type systems, planet formation modes should be similar to those in single star systems, with the secondary’s influence being roughly negligible (unless its orbit is sufficiently eccentric).

However, there are a handful of systems with detected planets where the secondary orbits at much closer separations (~ 20 au) - γ Cephei b (Hatzes et al. 2003), HD41004b (Zucker et al. 2004), GJ86b (Queloz et al. 2000), etc. The α Centauri system has similar orbital architecture, although as yet it does not host detections of exoplanets.

Despite this, the α Cen system is an attractive one for studying possible planet formation in binary systems. At a distance of 1.33

pc, it is the nearest star system to our Sun. It is composed of a hierarchical triple system, with the central binary system (α Cen AB) orbited by the M dwarf Proxima Cen at sufficiently large distance to be negligible (Wertheimer & Laughlin 2006). α Cen A is type G2V with mass $M_A = 1.105 \pm 0.007 M_\odot$, and α Cen B is type K1V with mass $M_B = 0.934 \pm 0.007 M_\odot$. It is particularly amenable to relatively cheap radial velocity (RV) campaigns (Guedes et al. 2008), especially if the goal is to detect Earth-mass planets within the habitable zone of a solar-type star.

As Guedes et al. (2008) describe, there are several reasons why this is the case: firstly, both α Cen A and B are high metallicity stars, which would promote the existence of circumstellar discs with a high fraction of solid materials at early times (Wyatt et al. 2007), as well as deeper spectral lines for improved RV precision. α Cen B is particularly quiet in terms of chromospheric activity and acoustic p-wave oscillations, with a relatively strong potential RV signal due to its lower mass. The binary is inclined by only 11 degrees with respect to the line of sight, i.e. its inclination angle from face-on is $i = 79^\circ$. This ensures that $\sin i \approx 1$, and that the recovered planet mass from RV observations will be close to the true mass, provided that the planets form and remain in the same plane. Finally, its position in the sky (-60° declination) affords astronomers in the southern hemisphere the opportunity to observe the system for most of the year. If α Cen B does host terrestrial

* E-mail: dhf@roe.ac.uk

¹ <http://exoplanet.eu/catalog.php>

planets, they should be readily detectable even with a 1 metre telescope with high-resolution spectrograph instrumentation.

Several numerical studies have shown that both stars are capable of forming terrestrial planets despite the perturbing influence of the binary companion, which appears to play a role analogous to the gas giants within our solar system. The planetesimal discs appear to be stable within 3 AU of their parent stars, provided the inclination of the disc relative to the binary plane is less than 60 degrees (Wiegert & Holman 1997; Quintana et al. 2002, 2007). However, other studies have shown that the later stages of accretion to produce lunar mass objects is reduced in efficiency due to orbital rephasing by the binary companion. This inhibits collisional growth around α Cen A to regions within 0.75 au (Th ebault et al. 2008), and within 0.5 au of α Cen B (Th ebault et al. 2009).

It therefore appears to be the case that gas giant formation is suppressed relative to our solar system (Xie et al. 2010), a prediction consistent with the absence of detections from previous radial velocity surveys, which suggest upper limits between 0.5 and 3 M_{Jup} . If the disc can produce a sufficient quota of lunar mass bodies, Guedes et al. (2008) show that Earth mass planets can form in the habitable zone of α Cen B, with maximum eccentricities of around $e_P = 0.3$ (this result is also corroborated by Xie et al 2010).

Once formed, Hamiltonian analysis indicates terrestrial planets orbiting in α Cen B’s habitable zone appear to be dynamically stable under perturbations from α Cen A, provided that $e_p < 0.3$ and the inclination of the planet’s orbit relative to the binary plane, $i_p < 35^\circ$ (Michtchenko & Porto de Mello 2009). Equally, these authors also show that planets with inclinations larger than this value are expected to experience strong instability due to the Lidov-Kozai resonance resulting in eccentricity-inclination coupling.

These studies have generally assumed a habitable zone (HZ) around α Cen B in the semi major axis range $0.5 < a < 0.9$ au. This range is based on calculations by Kasting et al. (1993), who calculate the HZ using a global radiative balance (GRBM) model, assuming Earth mass planets with similar atmospheric composition ($\text{N}_2/\text{H}_2\text{O}/\text{CO}_2$). The inner edge of the HZ is governed by loss of water via photolysis and subsequent hydrogen escape, and the outer edge is determined by formation of CO_2 clouds, which increase the planet’s albedo. In defining the habitable zone in this fashion, the perturbing influence of α Cen A is neglected. Given the semimajor axis of the orbit, this would appear to be an appropriate approximation. If main sequence relations for the luminosity of each object are assumed, the insolation experienced by planets in the habitable zone of α Cen B due to α Cen A would be no more than a few percent of the total insolation of the α Cen AB system at the binary’s periastron, and around one tenth of a percent at apastron. This insolation can be diminished further by eclipses of α Cen A by α Cen B, the duration of which is estimated to be of order a few Earth days.

However, we should also consider the results of more complex 1D latitudinal energy balance models (LEBMs) such as those described by Williams & Kasting (1997) and subsequently Spiegel et al. (2008, 2009); Dressing et al. (2010); Spiegel et al. (2010). Rather than pursuing a simple global balance, the planet’s temperature is allowed to vary as a function of latitude, λ . The insolation of the planet will also be a function of latitude and season, and the other key properties (infrared cooling rate and albedo) are also temperature dependent.

A planet in global radiative balance is not in general in local radiative balance, and by extension habitability is not a discrete concept (i.e. either habitable or uninhabitable), but a continuous one, where a certain fraction of the planet’s surface will be habit-

able at any given time. In the LEBM, the evolution of the planet’s temperature $T(\lambda)$ is described by a diffusion equation made non-linear by the addition of the heating and cooling terms, as well as an albedo which makes a rapid transition from low to high as temperature decreases past the freezing point of water. As a result, small changes in the properties of a planet can strongly affect the resultant climate. For example, changing the length of day in an Earth-type model can determine whether the planet can retain liquid water on the surface, or undergo an albedo feedback reaction which results in the “Snowball Earth” scenario (Spiegel et al. 2008).

These models have been successful in establishing important aspects of astronomical forcings on climate, e.g. Milankovitch cycles (Spiegel et al. 2010), variations due to orbital eccentricity, and potentially the effects of Kozai resonances or other orbital instabilities. It is this propensity for incorporating external forcing (such as the presence of a binary companion) which lends it towards studying habitability in systems such as α Cen AB. The sensitivity of the climate to such forcings suggest that the relatively small perturbation produced by the presence of α Cen A may have important consequences for the location of the habitable zone around α Cen B.

In this work, we augment the 1D LEBM of Spiegel et al. (2008) to include the presence of a binary companion, and perform a parameter study for planets orbiting α Cen B. In particular, we investigate the currently defined habitable zone, to compare with the GRBM calculations of Kasting et al. (1993). Section 2 describes our modified LEBM, and the initial conditions studied in the parameter space survey. Section 3 displays the results of this study. In section 4 we discuss the implications of these results, and summarise the work in section 5.

2 METHOD

2.1 Latitudinal Equilibrium Balance Models

At their core, LEBMs solve the following diffusion equation:

$$C \frac{\partial T(x, t)}{\partial t} - \frac{\partial}{\partial x} \left(D(1 - x^2) \frac{\partial T(x, t)}{\partial x} \right) = S(1 - A(T)) - I(T), \quad (1)$$

where $T = T(x, t)$ is the temperature at $x = \sin \lambda$, and λ is the latitude (between -90° and 90°). This equation is evolved with the boundary condition $\frac{\partial T}{\partial x} = 0$ at the poles. The $(1 - x^2)$ term is a geometric factor, arising from solving the diffusion equation in spherical geometry.

C is the effective heat capacity of the atmosphere, D is a diffusion coefficient that determines the efficiency of heat redistribution across latitudes, S is the insolation flux, I is the IR cooling and A is the albedo. In the above equation, C, S, I and A are functions of x (either explicitly, as S is, or implicitly through $T(x)$).

D is a constant, defined such that a planet at 1 au around a star of $1M_\odot$, with diurnal period of 1 day will reproduce the average temperature profile measured on Earth. Planets that rapidly rotate experience inhibited latitudinal heat transport, due to Coriolis effects (see Farrell 1990). In the model, we follow Spiegel et al. (2008) by scaling D according to:

$$D = 5.394 \times 10^2 \left(\frac{\omega_d}{\omega_{d,\oplus}} \right)^{-2}, \quad (2)$$

where ω_d is the rotational angular velocity of the planet, and $\omega_{d,\oplus}$ is the rotational angular velocity of the Earth. This expression is probably too simple to describe the full effects of rotation, but in the

absence of a first-principle theory to describe that describes reduced transport we must make do.

In this work, we solve the diffusion equation using a simple explicit forward time, centre space finite difference algorithm. A global timestep was adopted, with constraint

$$\delta t < \frac{(\Delta x)^2 C}{2D(1-x^2)}. \quad (3)$$

The parameters are diurnally averaged, i.e. a key assumption of the model is that the planets rotate sufficiently quickly relative to their orbital period. We adopt the same expressions for these parameters as Spiegel et al. (2008), who in turn used the work of Williams & Kasting (1997).

The atmospheric heat capacity depends on what fraction of the planet's surface is ocean, f_{ocean} , what fraction is land $f_{land} = 1.0 - f_{ocean}$, and what fraction of the ocean is frozen f_{ice} :

$$C = f_{land}C_{land} + f_{ocean}((1 - f_{ice})C_{ocean} + f_{ice}C_{ice}). \quad (4)$$

The heat capacities of land, ocean and ice covered areas are

$$C_{land} = 5.25 \times 10^9 \text{ erg cm}^{-2} \text{ K}^{-1} \quad (5)$$

$$C_{ocean} = 40.0C_{land} \quad (6)$$

$$C_{ice} = \begin{cases} 9.2C_{land} & 263 \text{ K} < T < 273 \text{ K} \\ 2C_{land} & T < 263 \text{ K}. \end{cases} \quad (7)$$

The infrared cooling function is

$$I(T) = \frac{\sigma_{SB}T^4}{1 + 0.75\tau_{IR}(T)}, \quad (8)$$

where the optical depth of the atmosphere

$$\tau_{IR}(T) = 0.79 \left(\frac{T}{273 \text{ K}} \right)^3. \quad (9)$$

The albedo function is

$$A(T) = 0.525 - 0.245 \tanh \left[\frac{T - 268 \text{ K}}{5 \text{ K}} \right]. \quad (10)$$

This produces a rapid shift from low albedo to high albedo as the temperature drops below the freezing point of water. It is this transition that makes the outer habitable zone extremely sensitive to changes to various orbital and planetary parameters, and makes LEBMs an important tool in studying short-term temporal evolution of planetary climates. The insolation flux S is a function of both season and latitude. At any instant, the bolometric flux received at a given latitude at an orbital distance r is

$$S = q_0 \cos Z \left(\frac{1 \text{ AU}}{r} \right)^2, \quad (11)$$

where q_0 is the bolometric flux received from the star at a distance of 1 AU, and Z is the zenith angle:

$$q_0 = 1.36 \times 10^6 \left(\frac{M}{M_\odot} \right)^4 \text{ erg s}^{-1} \text{ cm}^{-2} \quad (12)$$

$$\cos Z = \mu = \sin \lambda \sin \delta + \cos \lambda \cos \delta \cos h. \quad (13)$$

We have assumed main sequence scaling for the luminosity (M_\odot represents one solar mass). Given that both α Cen A and B are similar in mass (and spectral type) to the Sun, this is a reasonable first approximation, however, we should note the observational constraints placed by Thévenin et al. (2002), as we will in the Discussion. δ is the solar declination, and h is the solar hour angle. The solar declination is calculated from the obliquity δ_0 as:

$$\sin \delta = -\sin \delta_0 \cos(\phi_p - \phi_{peri} - \phi_a), \quad (14)$$

where ϕ_p is the current orbital longitude of the planet, ϕ_{peri} is the longitude of periastron, and ϕ_a is the longitude of winter solstice, relative to the longitude of periastron.

We must diurnally average the solar flux:

$$S = q_0 \bar{\mu}. \quad (15)$$

This means we must first integrate μ over the sunlit part of the day, i.e. $h = [-H, +H]$, where H is the radian half-day length at a given latitude. Multiplying by the factor H/π (as $H = \pi$ if a latitude is illuminated for a full rotation) gives the total diurnal insolation as

$$S = q_0 \left(\frac{H}{\pi} \right) \bar{\mu} = \frac{q_0}{\pi} (H \sin \lambda \sin \delta + \cos \lambda \cos \delta \sin H). \quad (16)$$

The radian half day length is calculated as

$$\cos H = -\tan \lambda \tan \delta. \quad (17)$$

We calculate habitability indices in the same manner as Spiegel et al. (2008). The habitability function η is:

$$\eta(\lambda, t) = \begin{cases} 1 & 273 \text{ K} < T(\lambda, t) < 373 \text{ K} \\ 0 & \text{otherwise.} \end{cases} \quad (18)$$

We then average this over latitude to calculate the fraction of habitable surface at any timestep:

$$\bar{\eta}(t) = \frac{\int_{-\pi/2}^{\pi/2} \eta(\lambda, t) \cos \lambda d\lambda}{2}. \quad (19)$$

We will use this function to classify the planets we simulate in the following sections.

2.2 Modifications to include the binary

The addition of the second star requires us to repeat the insolation flux calculation, where we must now re-calculate the orbital longitude, solar declination and radian half-day length of the planet relative to the secondary, and use the current the orbital distance from the planet to the secondary.

We must also account for the possibility of transits. Given the orbital configuration, transits of the secondary (α Cen A) by the primary (α Cen B) should occur frequently in the simulation. By calculating the angle between the vector \mathbf{r}_{21} between the two stars, and the vector \mathbf{r}_{p1} between the planet and the primary, it can be determined whether a transit is occurring at any given timestep². If the primary transits the secondary, the secondary flux is set to zero.

We ensure that transits are resolved in time by adding a second timestep criterion, which ensures that at the planet's current orbital velocity, the duration of a transit will not be less than 10 timesteps. We neglect the distant companion Proxima Centauri.

2.3 Initial Conditions

Unless otherwise stated, Earthlike conditions are assumed. The diurnal period is equal to the Earth's, and the obliquity is set to 23.5° . f_{ocean} is set to 0.7.

The α Cen system is set up to have $M_1 = M_B = 0.934M_\odot$,

² We also assume the stellar radii are governed by main sequence relations, see Prialnik (2000)

4 D. Forgan

$M_2 = M_A = 1.1M_\odot$. The semimajor axis of the orbit is $a = 23.4$ au, and the eccentricity $e = 0.5179$. α Cen A is placed at apastron at the beginning of all simulations.

In line with the results of Guedes et al. (2008), we investigate planet eccentricities between $e_p = 0$ to $e_p = 0.3$, and semi major axes relative to α Cen B in the conventionally established habitable zone $0.5 < a < 0.9$.

The simulations begin at the northern winter solstice, which is assumed to occur at an orbital longitude of 0° . In the case of eccentric orbits, this is also the longitude of periastron³. The planets' initial temperature was 288 K globally (starting the simulation at higher temperatures did not significantly affect the result). The simulations were carried out for 1000 years (approximately 15 orbits of α Cen A around α Cen B). The first 200 years of simulation are ignored, allowing the system to settle down to a quasi-steady state in all cases.

3 RESULTS

3.0.1 The Habitable Zone

Figure 1 shows the end result for all simulations carried out in this work. The various end states can be classified thus:

- (i) Habitable Planets - these planets are 100% habitable across the entire surface, i.e. $\bar{\eta}(t) = 1$ for all t .
- (ii) Hot Planets - these planets have temperatures above 373 K across all seasons, and are therefore uninhabitable ($\bar{\eta}(t) = 0$ for all t).
- (iii) Snowball Planets - these planets have undergone a snowball transition to a state where the entire planet is frozen, and are therefore uninhabitable ($\bar{\eta}(t) = 0$ for all t).
- (iv) Eccentric Transient Planets - these planets are partially habitable ($0 < \bar{\eta}(t) < 1$), but the habitability fraction oscillates according to the period of the planet's orbit around α Cen B. This oscillation is not present in circular orbits.
- (v) Binary Transient Planets - these planets are partially habitable ($0 < \bar{\eta}(t) < 1$), but the habitability oscillates with the period of α Cen A. This oscillation is present in both circular and eccentric orbits.

Some systems exhibit both types of transient behaviour. Where this is the case, we classify systems according to which oscillation has the largest amplitude.

If we instead chose to classify by maximum temperature, then most systems would be regarded as binary transients. Even planets in the middle of the habitable zone will experience temperature fluctuations. The resulting temperature oscillations due to α Cen A are quite small - the maximum temperature generally fluctuates by at most 2K.

Figure 2 shows the total fraction of the planet which is habitable, $\bar{\eta}(t)$, time-averaged over the range [300, 400] years. The steep gradient at the outer edge of the HZ indicates the non-linear, highly sensitive nature of the snowball transition. For single-star models using parameters corresponding to Earth and the Sun, $\bar{\eta} \approx 0.85$. Around α Cen B, planets on circular orbits will attain similar val-

³ Simulations were carried out where the longitude of periastron was varied. The results were not significantly affected, as the eccentricities studied are relatively low, see Dressing et al. (2010)

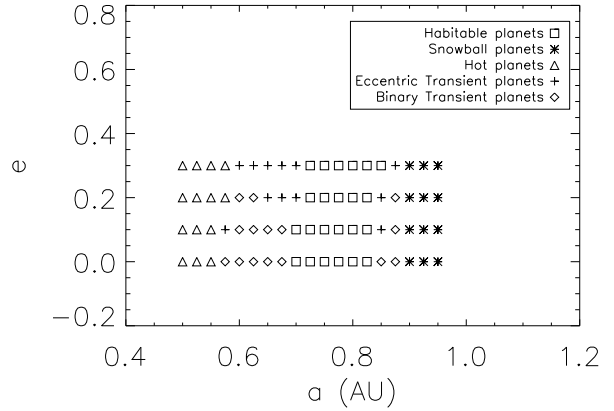


Figure 1. The habitable zone around α Cen B. The x-axis shows the semi-major axis of the planet orbiting α Cen B, the y-axis shows the eccentricity of the planet's orbit. The resulting planets are classified into five categories, which are described in the text.

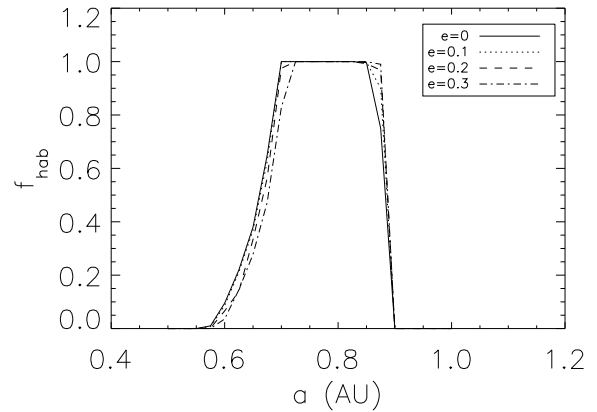


Figure 2. Habitability Fraction as a function of planet semi-major axis, time averaged in the date range [300, 400] years. Curves are plotted for four values of the planet's orbital eccentricity.

ues at $a_p = 0.86$ au⁴. This plot would indicate that the inner HZ would begin nearer to 0.6 than 0.5 au, with the edge of the outer HZ agreeing with previous results.

3.1 Habitable, Hot and Snowball Planets

Planets in these three categories have stable values of η throughout the season. The influence of α Cen A tends to raise the temperature by a few K at all eccentricities, with this phenomenon insensitive to any resonances between the longitude of periastron of the star and planet.

Temperature profiles (time averaged over one orbit of the planet) take essentially the same shape, of the form

$$T(\lambda) = A - B \sin^2 \lambda \quad (20)$$

With the snowball planets taking the lowest value of B , and the hot planets taking the largest values of B .

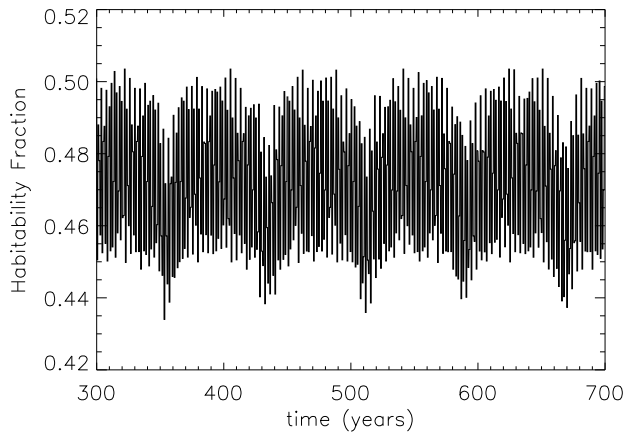


Figure 3. Habitability fraction as a function of time for the case where $a_p = 0.675$, $e_p = 0.3$.

3.2 Eccentric Transience

As was found by Dressing et al. (2010), eccentric planets are generally hotter compared to planets in circular orbits at the same semi-major axis (as received flux scales as $(1 - e^2)^{-1/2}$). As the eccentricity regime we explore is fairly modest, we do not see planets entering and leaving the snowball state purely because of high e_p . The planets do not spend long time intervals at apastron (relatively speaking), and therefore would not be able to freeze except if the semimajor axis was already sufficiently large.

Figure 3 shows $\bar{\eta}(t)$ in the case where $a_p = 0.675$ and $e_p = 0.3$. The variations due to the planet’s orbit are clearly visible as rapid fluctuations with amplitude of approximately 0.02. While eccentricity is the principal source of fluctuations here, the influence of α Cen A is clearly visible (e.g. at $t \sim 350$ years), reducing the habitable fraction by ~ 0.01 . In this example, equatorial latitudes exhibit temperatures above the boiling point of water - the passage of α Cen A increases the thickness of this inhospitable band.

3.3 Binary Transience

If we now take the previous example and set $e_p = 0$, then we can see the influence of α Cen A begin to dominate (left panel of Figure 4). The fluctuations due to eccentricity have effectively disappeared, and periastron passage of α Cen A (right panel of Figure 4 induces sharp decreases in $\bar{\eta}(t)$ of around 0.025. This clearly shows the habitability of the planet being significantly affected by α Cen A. This is despite the ratio of mean insolation from the primary and secondary, $\frac{S_2}{S_1} \leq 0.01$.

4 DISCUSSION

4.1 Dependence on the Secondary’s Orbit

We have focused specifically on the α Cen system in this paper. It is instructive to investigate other putative binary systems, to investigate the varying strength of binary perturbations. As the parameter space of binary star systems is quite large, we restrict ourselves to

⁴ The same value is achieved at $a_p = 0.69$ au, but this solution has no ice caps, and an equatorial $T > 373$ K

varying the orbital parameters of α Cen A, (a_2, e_2) , and assume the entire system is coplanar. Figure 5 shows how a planet’s minimum, maximum and global mean temperature varies as a_2 is decreased (with e_2 held at 0.5179). The planet parameters are fixed at $a_p = 0.9$, $e_p = 0$.

Taking the true orbital parameters of α Cen A (bottom right of figure), we can see that this is indeed a snowball planet, with the maximum temperature never exceeding 210 K. A slight perturbation in the mean can be seen at $t \sim 350$ years due to passage of α Cen A through periastron. Decreasing a_2 also decreases the orbital period; this can be seen in the other panels of Figure 5, with the minimum $a_2 = 5$ au (top left). More periastron passages induce more temperature fluctuations, but these are unable to melt the planet from its snowball state, with the exception of $a_2 = 5$ au (which produces mean temperatures close to terrestrial values). This climate cycle is stable over the entire simulation time. In this configuration, the insolation produced by α Cen A constitutes nearly a third of the total insolation by both stars at periastron, and around ten percent of the total insolation at apastron, so it is not entirely surprising that the planet can escape the snowball state.

Whether the outer HZ is extended or not depends quite sensitively on a_2 . We can see that $a_2 = 6$ au (top right) fails to melt the planet, despite producing temperature fluctuations of order 10 K. The insolation due to α Cen A is still approximately a third of the total energy budget at periastron, but the reduced frequency of periastron passages due to orbital distance means the time-averaged insolation is lower. This very small change in the magnitude and frequency of the perturbation induced by α Cen A is sufficient to completely alter the state of the planet in orbit around α Cen B from habitable to snowball.

In the habitable case shown here, the periastron of α Cen A is approximately 2.4 au. Can we produce another habitable planet by maintaining this periastron and α Cen A’s true semi major axis, $a_2 = 23.23$ au? This would correspond (roughly) to an eccentricity of $e_2 = 0.9$. As the periastron passage is now quite rapid, we should also expect that the climate model will become much more sensitive to the phase between the planet’s orbit and α Cen A’s. We investigate the dependence on phase by running the same simulation with different initial planetary orbital longitudes ($\phi_p = 0^\circ, 90^\circ, 180^\circ$).

The results can be seen in Figure 6. We can see that the planet remains in a snowball state, but experiences temperature fluctuations as large as 20 K. The strength of the fluctuations clearly varies with the relative position of planet and secondary as periastron is reached - each of the three plots shows the same behaviour, but with a phase shift caused by the planet’s shifted starting position. The perturbation in insolation due to α Cen A retains its maximum value at insolation of around 30% of the total, but the orbital period remains too long for these close passages to be sufficiently frequent to melt the planet.

4.2 Dependence on Ocean Fraction

We have assumed that the planets have the same surface ocean cover as Earth. Planets with lower ocean fractions are subject to shorter thermal relaxation timescales, and therefore will experience greater seasonal variations (Spiegel et al. 2008). It might therefore be reasonable to assume that drier planets will be more sensitive to binary fluctuations than wetter planets. This indeed appears to be the case, as is shown in Figure 7. We display habitability fractions for the same planetary parameters as Figure 4 with f_{ocean} now 0.1. The seasonal variations are substantially higher, with the fluctua-

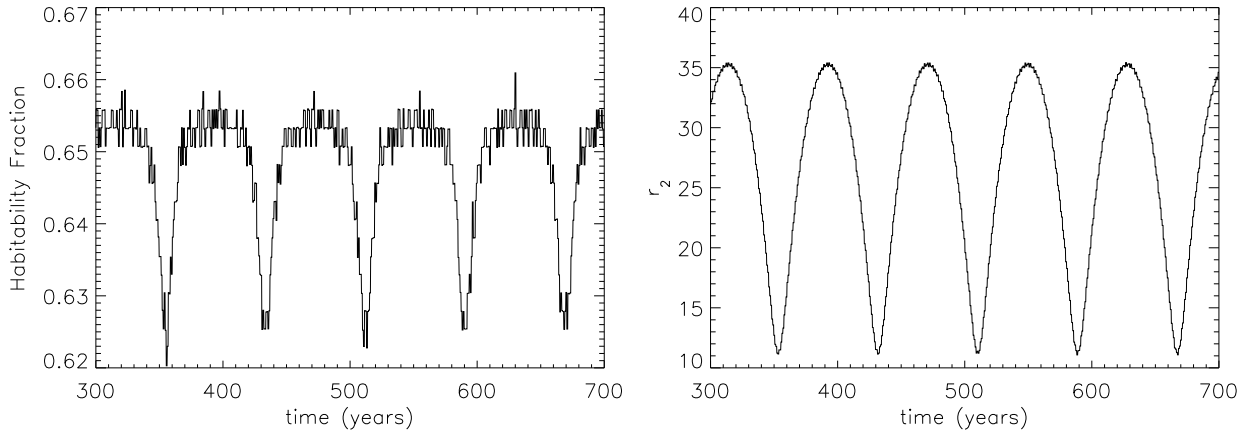


Figure 4. Left: Habitability fraction as a function of time for the case where $a_p = 0.675$, $e_p = 0.0$. Right: distance between the secondary and the planet as a function of time for the same planet parameters.

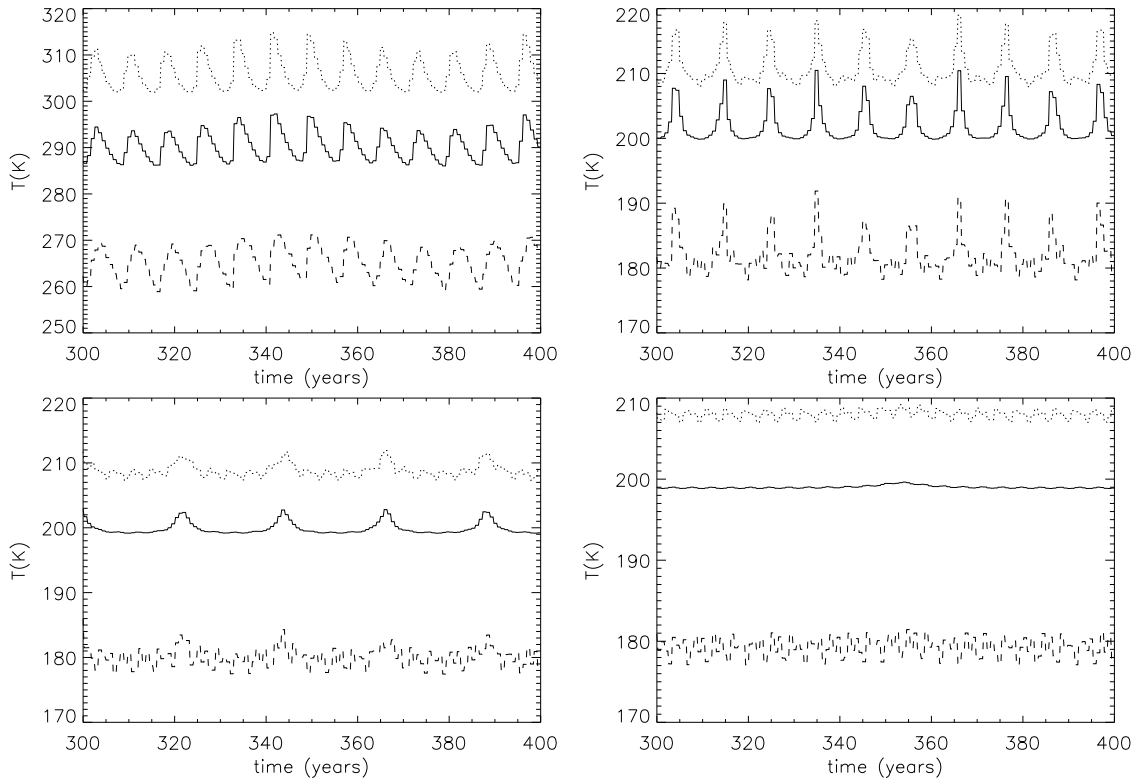


Figure 5. Comparing planet temperature as a function of time as the semi major axis of α Cen A is changed (for a planet with $a_p = 0.9$, $e = 0$). Top left shows $a_2 = 5AU$, top right shows $a_2 = 6AU$, bottom left shows $a_2 = 10AU$, and bottom right shows the true α Cen A semi major axis of 23.23 AU. The solid line indicates the global mean temperature, the dashed line the minimum temperature, and the dotted line is the maximum temperature.

tions due to α Cen A also slightly increased (from 0.025 to about 0.03).

4.3 Dependence on Obliquity

The influence of α Cen A adds a second seasonal variation to planets around α Cen B, with the polar declination varying in a non-trivial fashion over the period of the binary's orbit. How will binary oscillations alter under a change in obliquity? We have used the terrestrial value of 23.5° until this point, but there is no reason to discount other values. In our Solar System, Mars' obliquity appears to

have varied significantly between 0° and 60° (Laskar & Robutel 1993). In the case of Earth, the Moon has played an important role in stabilising obliquity fluctuations (Neron de Surgy & Laskar 1997), but this is not necessarily a general result for terrestrial planets with relatively large moons.

The influence of a binary can help lock the planet's obliquity into a so-called Cassini state (Correia et al. 2011). While these are generally low obliquity states, high obliquity states can also occur (Dobrovolskis 2009). Even without binary influence, numerical simulations indicate that the distribution of terrestrial planet obliq-

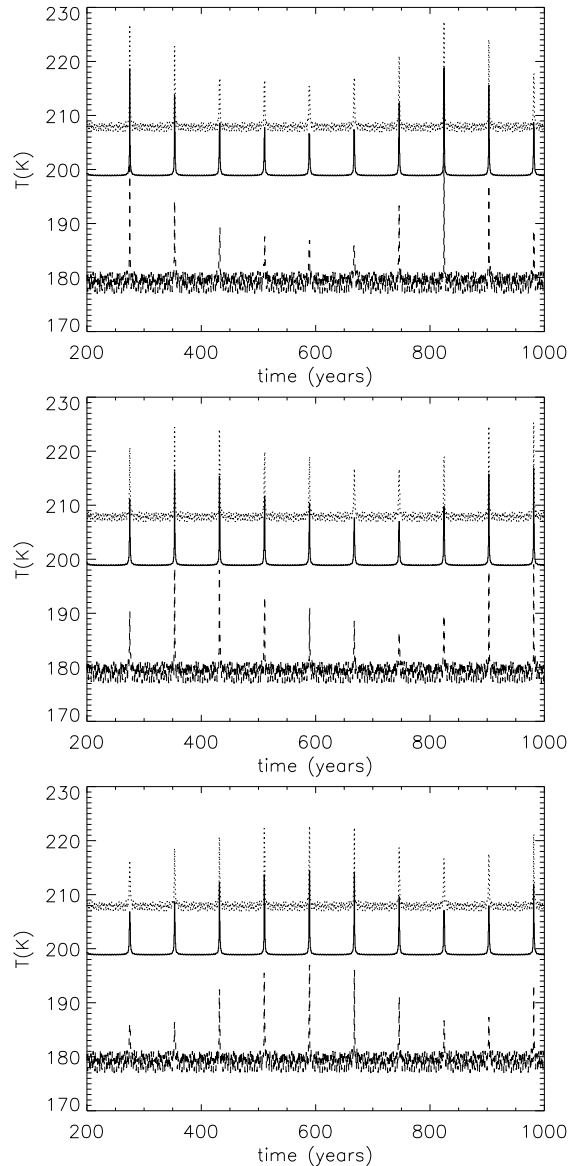


Figure 6. Comparing planet temperature as a function of time with the eccentricity of α Cen A, boosted to $e_2 = 0.9$ (for a planet with $a_p = 0.9$, $e = 0$). Top shows the starting orbital longitude of the planet $\phi = 0^\circ$, middle shows $\phi = 90^\circ$, and bottom shows $\phi = 180^\circ$.

uity is isotropic, and therefore primordial obliquities may be large (Kokubo & Ida 2007; Miguel & Brunini 2010).

Spiegel et al. (2009) show that high obliquity planets experience stronger seasonal variations, and can move far from global radiative balance even in circular orbits. While they are not necessarily more prone to snowball transitions, we may expect them to be more sensitive to binary fluctuations.

We investigate two other values of obliquity for the case where $a_p = 0.675$ au, $e_p = 0$, increasing the obliquity to 45° and 90° (Figure 8). The amplitude of the temperature oscillations are unaffected, but the temperatures themselves change significantly. Indeed, in the case of 45° spin, the planet requires re-classification from a binary transient to a habitable planet. This change (in line with the results of Spiegel et al. 2009 for single-star systems) underlines the difficulty of classifying planets as habitable or otherwise, as the parameter space for habitability is non-trivial and high in dimension.

4.4 Dependence on Rotation Rate

Other than convenience, there are no real reasons to assume that planets around α Cen B possess the same diurnal period as Earth.

We investigate planets rotating with 8, 24 and 72 hour periods (with $a_p = 0.675$, $e_p = 0$). Figure 9 shows the resulting minimum, maximum and mean temperatures as a function of time for all three cases. The temperature fluctuation induced by α Cen A maintains the same amplitude regardless of rotation rate.

Reducing the rotation period reduces heat transport, causing the radiant energy deposited by the primary to be diffused to a smaller range of latitudes, increasing the temperature gradient in the fast rotating case (top panel of Figure 9). The slower rotating case shows the more efficient latitudinal transport distributing insolation such that the temperature range from pole to pole is less than 20K (bottom panel).

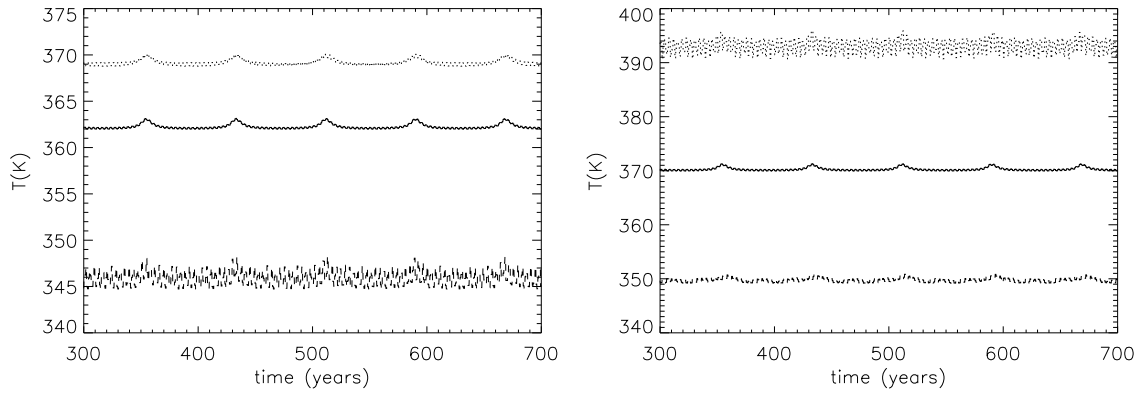


Figure 8. Comparing planet temperature as a function of time as the obliquity of the planet is changed (for a planet with $a_p = 0.675$, $e = 0$). The left hand plot shows a planet with with obliquity increased to 45° , and the right hand plot shows a planet with obliquity increased to 90° . The solid line indicates the global mean temperature, the dashed line the minimum temperature, and the dotted line is the maximum temperature.

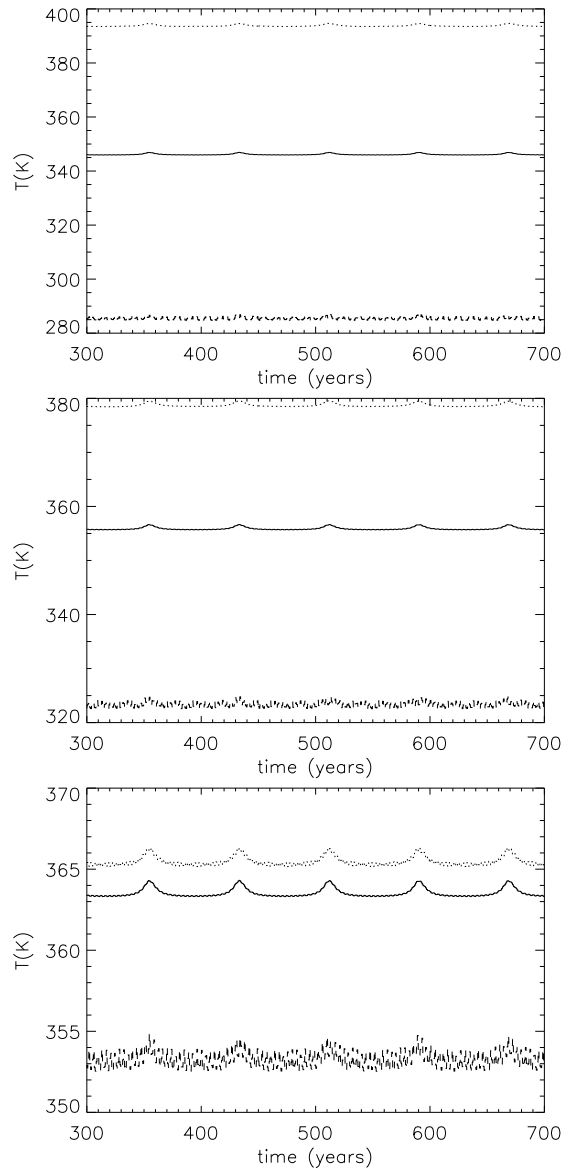


Figure 9. Comparing planet temperature as a function of time as the diurnal period of the planet is changed (for a planet with $a_p = 0.675$, $e = 0$). The left hand plot shows a planet with diurnal period equal to one day, and the right hand plot shows a planet with diurnal period equal to a third of a day. The solid line indicates the global mean temperature, the dashed line the minimum temperature, and the dotted line is the maximum temperature.

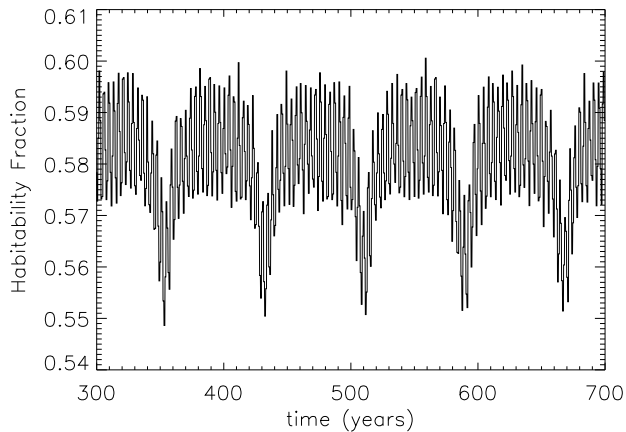


Figure 7. Habitability fraction as a function of time for the case where $a_p = 0.675$, $e_p = 0.0$, and the fraction of planet surface which is ocean, $f_{ocean} = 0.1$.

4.5 Limitations of the Model

Finally, we should note the limitations of the above analyses. As with the work of Spiegel et al. (2008), the 1D LEBM can only capture a restricted range of thermal timescales. While it is sensitive to seasonal forcing and (as a result) orbital timescales, the model does not exhibit the features of much slower climate processes, which possess timescales many times the orbital period of the α Cen system. For example, oceanic circulation is not included in this model, which can determine longer-term climate variation.

More complex additions, such as clouds and a carbonate-silicate cycle (e.g. Williams & Kasting 1997) would provide a further regulating effect on planet temperatures, potentially extending the outer edge of the habitable zone (Kasting et al. 1993) on long enough timescales. In the particular case of binary systems, we might expect that the oscillations induced by the presence of a companion would be damped, if the silicate cycle can respond sufficiently quickly during periastron passage. The timescale on which the silicate cycle can be expected to respond is sensitive to the specific properties of the planet, i.e. its chemistry, geology and ocean circulation systems. For the Earth, it has been estimated that the equilibration timescale for the carbonate-silicate cycle is around 0.5 Myr (Williams & Kasting 1997). A more rapid means of CO_2 release may be through warming the oceans, as their capacity to hold CO_2 decreases with increasing temperature. The relevant timescale would instead be ocean circulation timescales, which are of the order 10^3 years. Again, these timescales are representative for the Earth only, and will not apply in general to terrestrial exoplanets.

Perhaps the most obvious limitation of these models is their dimension. 1D modelling prevents discussion of longitudinal climate variations, and forces us to consider diurnally averaged insolation. This prevents simulation of planets with slow rotation rates relative to their orbital motion (such as Venus, see Parish et al. 2011). The contrast between land and ocean is also lost in 1D, and latitudinal variations that occur as a result are not accounted for. Despite this, 1D LEBMs still capture much of the relevant physics, capable of reproducing fiducial Earths with temperature profiles very similar to real data (Spiegel et al. 2008). The inner edge of the habitable zone is less well-defined than the outer edge - atmospheric changes could allow liquid water above 373 K, and the runaway greenhouse effect may become important at temperatures nearer 350 K (Spiegel et al. 2008 and references within). In any case, the outer edge is likely to be more interesting from an astrobiological

standpoint, as current and future instrumentation will be more capable of probe spectral features of planets at larger semi-major axes (see e.g. Kaltenegger & Selsis 2010).

We should acknowledge, however, that the addition of a second insolation source into diffusion approximation-based models such as this is not entirely understood. However, the perturbations induced by secondary insolation are relatively small (typically a few percent of the primary insolation, except in extreme cases). We therefore argue that the models are appropriate for an initial exploratory investigation.

Thévenin et al. (2002) estimate the luminosity of α Cen B as $0.5002 \pm 0.016L_{\odot}$, which differs from the main sequence value used in this work by around 30%. The habitable zone would be somewhat closer to the star as a result, increasing the number of planetary orbits per binary orbit. While much of the qualitative trends in this paper would remain unchanged, it is clearly important that future studies of habitability in this system use observationally constrained luminosities.

We should also note that we neglect the effect of α Cen A's gravitational field on the dynamics of α Cen B's planets. While the planet's orbital inclination is low enough to avoid Kozai resonances, and the mean motion resonances due to α Cen A are absent from the orbits we explore (Michtchenko & Porto de Mello 2009), we should still expect short period perturbations to the planet semi-major axis of order 0.01 au, more than sufficient to produce substantial Milankovitch cycles (Spiegel et al. 2010). We have seen that the outer edge of the HZ is sensitive to perturbations of this size, so future studies must incorporate these perturbations in more detail.

5 CONCLUSIONS

We have investigated the influence of α Cen A on the habitable zone of α Cen B, to test the efficacy of the single-star approximation in a binary context. In general, we demonstrate that the single-star approximation is roughly correct for calculating the inner and outer boundaries of the habitable zone, but fails to capture oscillations in the planet's climate that occur as a result of α Cen A's passage through periastron.

For all planetary orbits, the presence of α Cen A induces temperature fluctuations of order a few K. At the habitable zone boundaries, the fraction of habitable surface on such planets can be altered by around 3%. The strength of these fluctuations can be increased by reducing the planet's ocean fraction, or increasing its obliquity.

It is reasonable to speculate that if life were to exist on planets around α Cen B, that they may develop two circadian rhythms (cf Breus et al. 1995) corresponding to both the length of day around the primary, and the period of the secondary's orbit (approx 70 years). Altering the available habitat by a few percent may also influence migration patterns and population evolution.

While we have demonstrated that the temperature fluctuations for planets around α Cen B due to α Cen A are relatively small, the consequences of a periodic temperature forcing of a few K to long term climate evolution cannot be fully understood from this work. To fully appreciate the impact on (for example) ocean circulation and carbonate-silicate cycles requires further investigation with more advanced climate models.

ACKNOWLEDGMENTS

All simulations were performed using high performance computing funded by the Scottish Universities Physics Alliance (SUPA). DF gratefully acknowledges support from STFC grant ST/H002380/1. The author would like to thank Caleb Scharf for useful discussions, and the referee, David Spiegel, whose comments and insights greatly improved this manuscript.

REFERENCES

- Breus T. K., Cornéllissen G., Halberg F., Levitin A. E., 1995, *Annales Geophysicae*, 13, 1211
- Correia A. C. M., Laskar J., Farago F., Boué G., 2011, *Celestial Mechanics and Dynamical Astronomy*, 111, 105
- Desidera S., Barbieri M., 2007, *A&A*, 462, 345
- Dobrovolskis A. R., 2009, *Icarus*, 204, 1
- Dressing C. D., Spiegel D. S., Scharf C. A., Menou K., Raymond S. N., 2010, *ApJ*, 721, 1295
- Duquennoy A., Mayor M., 1991, *A&A*, 248, 485
- Farrell B. F., 1990, *Journal of Atmospheric Sciences*, 47
- Guedes J. M., Rivera E. J., Davis E., Laughlin G., Quintana E. V., Fischer D. A., 2008, *ApJ*, 679, 1582
- Hatzes A. P., Cochran W. D., Endl M., McArthur B., Paulson D. B., Walker G. A. H., Campbell B., Yang S., 2003, *ApJ*, 599, 1383
- Kaltenegger L., Selsis F., 2010, *EAS Publications Series*, 41, 485
- Kasting J., Whitmire D., Reynolds R., 1993, *Icarus*, 101, 108
- Kokubo E., Ida S., 2007, *The Astrophysical Journal*, 671, 2082
- Laskar J., Robutel P., 1993, *Nature*, 361, 608
- Michtchenko T., Porto de Mello G. F., 2009, *Bioastronomy 2007: Molecules*, 420
- Miguel Y., Brunini A., 2010, *Monthly Notices of the Royal Astronomical Society*, 406, no
- Neron de Surgy O., Laskar J., 1997, *A&A*, 318, 975
- Parish H. F., Schubert G., Covey C., Walterscheid R. L., Grossman A., Lebonnois S., 2011, *Icarus*, 212, 42
- Prialnik D., 2000, *An Introduction to the Theory of Stellar Structure and Evolution*. Cambridge University Press
- Queloz D., Mayor M., Weber L., Blécha A., Burnet M., Confino B., Naef D., Pepe F., Santos N., Udry S., 2000, *A&A*, 354, 99
- Quintana E. V., Adams F. C., Lissauer J. J., Chambers J. E., 2007, *ApJ*, 660, 807
- Quintana E. V., Lissauer J. J., Chambers J. E., Duncan M. J., 2002, *ApJ*, 576, 982
- Spiegel D. S., Menou K., Scharf C. A., 2008, *ApJ*, 681, 1609
- Spiegel D. S., Menou K., Scharf C. A., 2009, *ApJ*, 691, 596
- Spiegel D. S., Raymond S. N., Dressing C. D., Scharf C. A., Mitchell J. L., 2010, *ApJ*, 721, 1308
- Thébaud P., Marzari F., Scholl H., 2008, *MNRAS*, 388, 1528
- Thébaud P., Marzari F., Scholl H., 2009, *MNRAS*, 393, L21
- Thévenin F., Provost J., Morel P., Berthomieu G., Bouchy F., Carrier F., 2002, *Astronomy and Astrophysics*, 392, L9
- Wertheimer J. G., Laughlin G., 2006, *The Astronomical Journal*, 132, 1995
- Wiegert P. A., Holman M. J., 1997, *The Astronomical Journal*, 113, 1445
- Williams D., Kasting J. F., 1997, *Icarus*, 129, 254
- Wyatt M. C., Clarke C. J., Greaves J. S., 2007, *MNRAS*, 380, 1737
- Xie J.-W., Zhou J.-L., Ge J., 2010, *ApJ*, 708, 1566

Zucker S., Mazeh T., Santos N. C., Udry S., Mayor M., 2004, *A&A*, 426, 695